34th Annual International Conference of the IEEE EMBS
San Diego, California USA, 28 August - 1 September, 2012

A New Microfluidic Device for Electric Lysis and Separation of Cells

M. Brun*, M. Frénéa-Robin, J.F. Chateaux, N. Haddour, A.L. Deman and R. Ferrigno.

Abstract—**This paper demonstrates the potential use of a new microfluidic device embedding thick electrodes for cell lysis and cell separation applications. The system consists of a microfluidic channel featuring conductive walls made of a polydimethylsiloxane (PDMS) matrix mixed with carbon nanoparticles. Cell lysis was performed electrically by applying square pulses across the channel width, which was monitored by fluorimetry. Lysed and unlysed cells showed different dielectrophoretic behavior under appropriate experimental conditions, which suggests that the developed device is suitable to perform both cell lysis and subsequent sorting of viable and dead cells**

I. Introduction

Analysis of subcellular materials is essential for many fundamental biological studies [1][2]. It requires breaking the cell membrane which can be done using methods conventionally based on chemical (using surfactants), mechanical (for example using ultrasounds), thermal or electrical techniques [1]. The emergence of lab-on-chips dedicated to the manipulation of cells has quickly led to the production of devices dedicated to cell lysis. Microsystems have the benefits of direct environment control, unique cell handling and integration with other microfluidic functions such as biomolecules detection. Many devices are based on electroporation [3], *i.e.* creating transient (or not) pores through cell membranes under the effect of an external electric field. Cells are usually placed between two coplanar electrodes separated by a few hundreds of micrometers, which is particularly interesting in order to reach high electric fields from low tensions. However, this kind of electrodes can be oxidized or destroyed during experiments. Additionally, some works highlighted the relevance of thick electrodes to perform electrokinetic manipulations in microfluidics and particularly for cells lysis and trapping. Indeed this electrode configuration favors uniform lateral electric fields across the microchannel section [4][5]. Here we chose to use electrodes made of cPDMS, a nanocomposite material obtained by mixing PDMS (polydimethylsiloxane) and carbon nanoparticles [6][7][8]. Biocompatible and low cost, cPDMS can be structure by soft lithography and can also be irreversibly sealed to glass, PDMS and silicon substrates, which is not possible with conventional metallic electrodes.

* Supported by French Research Ministry.

M. Brun is postdoc at Ampère Lab, UMR5005 CNRS, Ecole Centrale de Lyon, 39134 Ecully Cedex, France (corresponding author) (+33)4-72186118; fax: (+33)4-72431193; mathieu.brun@ec-lyon.fr.

M. Frénéa-Robin and N. Haddour are assistant professor at Ampère UMR 5005 CNRS, respectively at Université Claude Bernard Lyon 1 and Ecole Centrale de Lyon, France.

A.L. Deman, assistant professor, J.F. Chateaux, assistant professor, and R. Ferrigno, professor, work at the Institut des Nanotechnologies de Lyon UMR 5270 CNRS, Université Claude Bernard Lyon 1, France.

II. Experimental Section

A. Microdevice fabrication

cPDMS was obtained by mixing 25% (wt) carbon nanopowder (Vulcan XC-72R, Cabot) with PDMS (Sylgard 184, Dow Corning). PDMS device was prepared using a double photolithography process as published previously [8]. It consists of a 200 µm wide microfluidic channel with 100 µm thick cPDMS electrodes (Fig. 1).

B. Cell preparation

HEK-293 cells (human embryonic kidney, ATCC CRL-1573™) obtained from PAA were grown in DMEM (Dulbecco's Modified Eagle's Medium) supplemented with 10% FBS (fetal bovine serum), 5% glutamine and 5% penicillin–streptomycin. Cells were incubated in a 5% CO_2/95% O_2 atmosphere at 37°C for two days. Buffer was prepared using 10 µM PBS (phosphate buffer saline), pH 7.4 using deionized water. This solution was supplemented with saccharose to set the osmolarity to 300 mOsm L^{-1}. At 80% confluence, cells were washed in DMEM, detached with trypsin, washed and resuspended few times in buffer. Then cell cytoplasm was labeled with 1% calcein AM (Sigma-Aldrich) before being injected into the microchannel using microfluidic control flow system (Fluigent).

C. Equipment

Electrodes were polarized using a waveform generator (Agilent 33250A) computer-controlled by Labview™ and coupled with a high speed bipolar amplifier (NF HSA 4011). Observations were made with a Nikon Eclipse LV150 microscope equipped with a digital video camera (Zeiss AxioCamHSm). Image acquisition was performed using Axiovision 4.6 software (Carl Zeiss, Inc.).

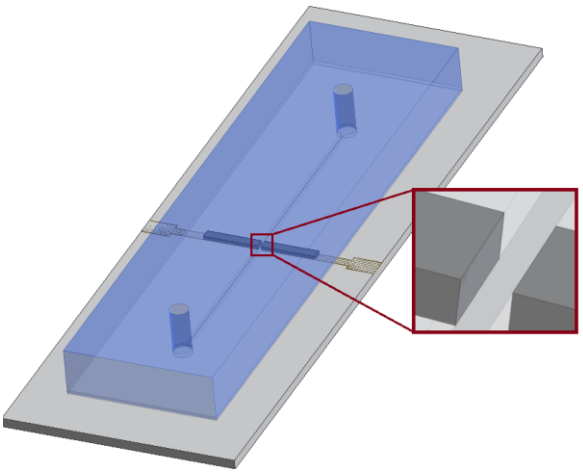

Figure 1. The microdevice is made of PDMS integrating two 100 µm-thick cPDMS electrodes spaced by 200 µm.

III. THEORY

Cell behavior under electric field depends on the suspension medium composition, on the electric field parameters and directly on the cell dielectric properties. Indeed, cells can be electrically described like a thin insulating lipid double-layer membrane surrounding conductive cytosolic material [9][10].

A. Electroporation

The accumulation of negatively charged molecules within the cell (Fig. 2.a) leads to a voltage difference across the cell membrane called transmembrane potential (TMP). The application of an external electric field (E) induces a potential difference ($\Delta\psi_i$) depending on the cell geometry according to the simplified Schwann relation [11]:

$$\Delta\psi_i = 1{,}5.E.a.\cos(\alpha) \quad (1)$$

where E denotes the magnitude of the field, a the cell radius, α represents the angle between the direction of E and the site on the cell membrane where $\Delta\psi_i$ is measured (Fig. 2.a).

Above a critical field (*Ec*, usually around 1 kV/cm [3]), pore formation (Fig. 2.b) is induced at the maximal field region ($cos\ \alpha = 1$), where the critical TMP (Ψc) is reached. With field increase, Ψc is progressively reached all around the cell (Fig. 2.c)[12]. Electroporation can be reversible, *i.e.* pores can reseal themselves when the field is stopped. But when the electrical field exceeds the irreversible permeabilization threshold, the membrane breaks down which leads to cell lysis.

B. Dielectrophoresis (DEP)

When the applied electric field is too low to induce electroporation, it can yet generate cell motion in particular by DEP. This phenomenon occurs when cells are exposed to non-uniform electric fields. DEP force is given by the expression:

$$F_{DEP} = 2\pi.\varepsilon_0.\varepsilon_m.a^3.Re[f_{CM}(\omega)].\nabla E^2 \quad (2)$$

Where a represents the cell radius, ε_0 the vacuum permittivity, ε_m the relative permittivity of the medium, and E the RMS field intensity. $Re[f_{CM}]$ is the real part of the Clausius-Mossotti factor namely the relation between dielectric properties of cell (c) and suspension medium (m) [13][14]:

$$f_{CM}(\omega) = \frac{\varepsilon_c^* - \varepsilon_m^*}{2\varepsilon_c^* + \varepsilon_m^*} \quad (3)$$

where ω denotes the angular frequency of the electric field, ε^* the complex permittivity ($\varepsilon^* = \varepsilon_0.\varepsilon - j\sigma/\omega$) and σ the conductivity.

When cells are less polarizable than the suspension medium ($Re[f_{CM}]<0$), the DEP force is negative (nDEP) and cells are repelled away from high field regions. Inversely, if cells are more polarizable than their suspension medium ($Re[f_{CM}]>0$), they move towards field maxima under the influence of positive DEP (pDEP). $Re[f_{CM}]=0$ at the so-called "cross-over" frequency [13][14].

IV. RESULTS AND DISCUSSION

A. DEP spectra of HEK-293 cells

Characterized by intrinsic properties, each kind of cell can be profiled by its specific dielectrophoretic spectrum which represents the evolution of its f_{CM} (real and imaginary parts) with respect to the frequency of the electric field. The real part describes cell polarisability while imaginary part provides information on dielectric loss [15]. Blue dashed line on Fig. 3 presents the HEK-293 DEP spectrum (real part) plotted using HEK-293 dielectric properties extracted from the literature [16] and the "single-shell" approximation of f_{CM} [17]. Under 50 kHz (cross-over frequency, Fig. 3), HEK-293 cells are subjected to nDEP as previously observed in our experimental studies [8]. Inversely at higher frequencies cells move towards the electrodes by pDEP.

It is important to notice that DEP force depends directly on the gradient of E (2), which implies that our electrode configuration (thick and parallel) is theoretically non favorable to DEP observations. However, as numerically demonstrated by Kua *et al* [18], the simple presence of cells induces electric field inhomogeneities sufficient to generate a DEP force. As stated by the authors, this effect increases with the number and size of cells and their proximity to electrodes. Moreover the roughness and the heterogeneity of electrodes, especially for composite materials, can increase the electric field gradient near the channel walls.

Some parameters of cells and suspension medium (such as the cell size, the medium conductivity, or cell membrane conductance) have a critical influence on the f_{CM} and therefore on the DEP spectra. Literature also reports consequences of cell lysis on their DEP spectra [19][20]. Membrane breakdown leads to leakage of cytosol into extracellular space and therefore impacts the cell conductivity.

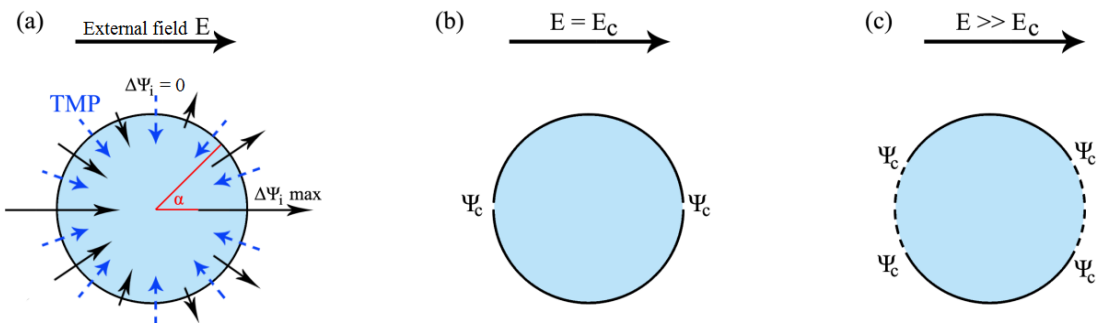

Figure 2. Picturing of cell electroporation principle. (a) External field induces electric potential difference ($\Delta\psi_i$) adding to the intrinsic TMP of the cell. (b) Increase of E leads to electroporation when critical potential (Ψc) is reached. (c) With field increase, pores are progressively formed all around the cell in accordance with Schwann relation (1).

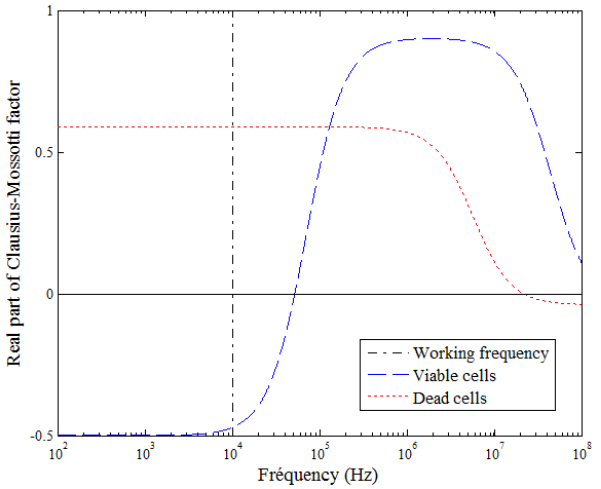

Figure 3. Dielectrophoretic spectra of viable HEK-293 cells (σ_m=10^{-2} S/m, ε_m=80, σ_c=0.533 S/m,ε_c=71, a=5.10^{-6} m, Cm=$8.5.10^{-3}$ F/m^{-2}) and dead HEK-293 (σ_c=0.053 S/m).

Red dotted line on Fig. 3 approximates the dielectrophoretic behavior of lysed HEK-293 cells. The f_{CM} formula was obtained from [19] and dielectric parameters estimated from the literature [21] and our fluorescent experiments (Fig. 4).

B. *Electrical lysis of HEK-293 cells*

Cell lysis depends on different electrical parameters such as number, amplitude or length of pulses. On the basis of previous studies reported in the literature [2][3], we chose to apply 4 pulses separated by 1 ms. Then we varied the pulse length (between 10 and 1000 µs) and their intensity (between 1 and $3.5.10^5$ V/m) in order to find the optimum conditions of cell lysis. Checkout of the lysis was performed using calcein AM. Monitoring of fluorescence during electroporation enabled to confirm cell lysis. Fig. 4 presents an example of the outflow of fluorescent dye consequently to the pulse application (here 3.10^5 V/m, 1 ms in length). Fluorescence intensities indicate that about 50% of calcein got out of the cell just 1 second after pulses (green dashed line). 5 minutes after electroporation (blue dotted line), we observed a decrease of around 80% of cytoplasm fluorescence. Control sample (data not shown) confirms that this effect does not come from quenching. Thereby we can estimate that a large

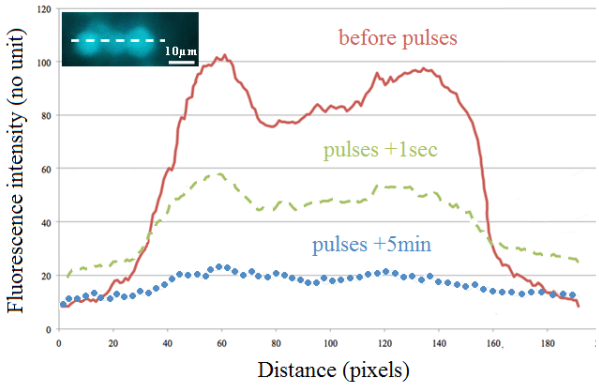

Figure 4. Evolution of fluorescence intensity during application of 4 pulses (3.10^5 V/m, 1 ms length) separated from 1 ms. HEK-293 cells were labeled with 1% calcein AM.

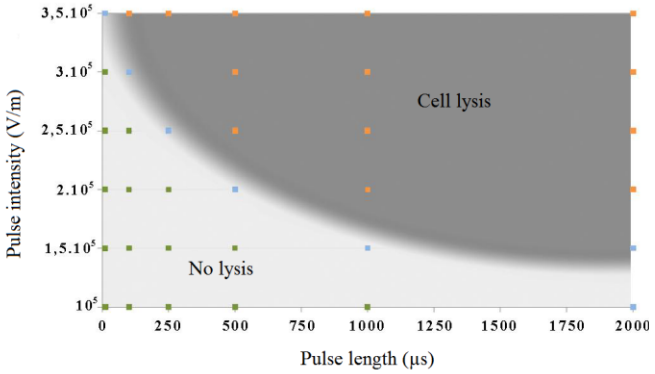

Figure 5. Lysis efficiency functions of length and intensity of 4 pulses separated by 1 ms.

proportion of cytoplasm has leaked from the cell. Considering the low conductivity of cell immersion medium, this probably leads to widely reduce cytosolic conductivity (σ_c).

Fig. 5 presents lysis threshold obtained from different pulses parameters (length and intensity). As expected, the shorter are the pulses, the higher intensity is needed to perform cell lysis. Inversely, when large pulses are applied, lower field intensities are sufficient to induce HEK-293 lysis. The borderline between lysis and no lysis is arbitrarily defined for 70% efficiency of cell lysis.

C. *DEP behavior of lysed and viable cells*

As can be expected from the dielectrophoretic spectra presented Fig. 3, lysed and unlysed cell can be separated thanks to their dielectric properties. Indeed, under the crossover frequency of viable cells (around 50 kHz), lysed cells are subjected to pDEP while viable cells experiments nDEP. So we chose to work with a frequency of 10 kHz, which is enough to distinguish both DEP behaviors and to avoid low-frequency phenomenons such as electroosmosis or electrolysis. Fig. 6.a presents viable cells subjected to an electric field of 10 kHz and 2.10^5 V/m. Cells were consequently aligned in the center of the microchannel in accordance with classical nDEP behavior. Then, cell lysis was performed using parameters obtained from Fig. 5. Following pulse application, lysed cells moved towards the electrodes showing typical pDEP behavior as presented Fig. 6.b. This last result demonstrates that the device could be used to perform lysed and unlysed cell separation using DEP.

V. Conclusion

In this paper, we demonstrated that HEK cell lysis could be successfully performed using nanocomposite carbon-PDMS thick electrodes embedded in a microfluidic channel. Such device was fabricated using a simple process based on soft-lithography. The modification of HEK dielectrophoretic behavior following cell lysis could be advantageously exploited to sort lysed and unlysed cells by using the same device. Indeed, unlysed cells experiencing negative dielectrophoresis could be driven by laminar flow towards a central channel outlet, while lysed cells attracted to the electrode walls would exit the channel by side outlets.

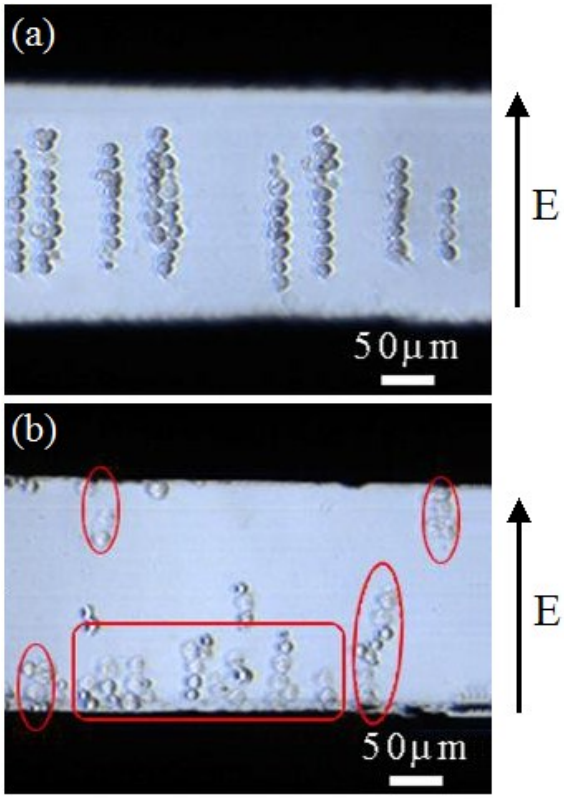

Figure 6. HEK-293 cells behavior under AC electric field of 10 kHz, 2.10^5 V/m before (a) and after (b) implementing of cell lysis.

ACKNOWLEDGMENT

This work was supported by a PEPS program from the CNRS. NanoLyon clean room facilities were used to fabricate themicrofluidic devices. The authors gratefully thank A. El Gaddar and O. Osman for cell culture preparation.

REFERENCES

[1] H. Andersson, "Microfluidic devices for cellomics: a review," *Sensors and Actuators B: Chemical*, vol. 92, no. 3, pp. 315-325, 2003.

[2] H. Lu, M. A. Schmidt, and K. F. Jensen, "A microfluidic electroporation device for cell lysis.," *Lab on a chip*, vol. 5, no. 1, pp. 23-9, Jan. 2005.

[3] S. Movahed and D. Li, "Microfluidics cell electroporation," *Microfluidics and Nanofluidics*, vol. 10, no. 4, pp. 703-734, Oct. 2010.

[4] T. Müller, G. Gradl, S. Howitz, S. Shirley, T. Schnelle, and G. Fuhr, "A 3-D microelectrode system for handling and caging single cells and particles," *Biosensors & bioelectronics*, vol. 14, no. 3, pp. 247-256, 1999.

[5] K.-Y. Lu, A. M. Wo, Y.-J. Lo, K.-C. Chen, C.-M. Lin, and C.-R. Yang, "Three dimensional electrode array for cell lysis via electroporation.," *Biosensors and Bioelectronics*, vol. 22, no. 4, pp. 568-574, 2006.

[6] M. Brun, J.-F. Chateaux, A.-L. Deman, P. Pittet, and R. Ferrigno, "Nanocomposite Carbon-PDMS Material for Chip-Based Electrochemical Detection," *Electroanalysis*, vol. 23, no. 2, pp. 321-324, Feb. 2011.

[7] X. Z. Niu, S. L. Peng, L. Y. Liu, W. J. Wen, and P. Sheng, "Characterizing and Patterning of PDMS-Based Conducting Composites," *Advanced Materials*, vol. 19, no. 18, pp. 2682-2686, Sep. 2007.

[8] A.-L. Deman et al., "Characterization of C-PDMS electrodes for electrokinetic applications in microfluidic systems," *Journal of Micromechanics and Microengineering*, vol. 21, no. 9, p. 095013, 2011.

[9] G. H. Markx and C. L. Davey, "The dielectric properties of biological cells at radiofrequencies: applications in biotechnology," *Enzyme and Microbial Technology*, vol. 25, no. 3-5, pp. 161-171, 1999.

[10] R. Pethig and D. B. Kell, "The passive electrical properties of biological systems: their significance in physiology, biophysics and biotechnology," *Physics in Medicine and Biology*, vol. 32, no. 8, pp. 933-970, Aug. 1987.

[11] K. A. DeBruin and W. Krassowska, "Modeling electroporation in a single cell. I. Effects Of field strength and rest potential.," *Biophysical journal*, vol. 77, no. 3, pp. 1213-24, Sep. 1999.

[12] U. Zimmermann and G. A. Neil, *Electromanipulation of Cells*. CRC-Press, 1996, p. 416.

[13] P. R. C. Gascoyne and J. Vykoukal, "Particle separation by dielectrophoresis.," *Electrophoresis*, vol. 23, no. 13, pp. 1973-83, Jul. 2002.

[14] R. Pethig, "Review Article-Dielectrophoresis: Status of the theory, technology, and applications.," *Biomicrofluidics*, vol. 4, no. 2, p. 022811, Jan. 2010.

[15] P. R. C. Gascoyne and J. V. Vykoukal, "Dielectrophoresis-Based Sample Handling in General-Purpose Programmable Diagnostic Instruments.," *Proceedings of the IEEE Institute of Electrical and Electronics Engineers*, vol. 92, no. 1, pp. 22-42, 2004.

[16] D. Zimmermann et al., "A combined patch-clamp and electrorotation study of the voltage- and frequency-dependent membrane capacitance caused by structurally dissimilar lipophilic anions.," *The Journal of membrane biology*, vol. 221, no. 2, pp. 107-21, Jan. 2008.

[17] V. Sukhorukov, "A single-shell model for biological cells extended to account for the dielectric anisotropy of the plasma membrane," *Journal of Electrostatics*, vol. 50, no. 3, pp. 191-204, 2001.

[18] C. H. Kua, C. Yang, S. Goh, R. Isabel, K. Youcef-Toumi, and Y. C. Lam, "Generation of Dielectrophoretic Force under Uniform Electric Field." 10-Jan-2006.

[19] C.-P. Jen and T.-W. Chen, "Selective trapping of live and dead mammalian cells using insulator-based dielectrophoresis within open-top microstructures," *Biomedical Microdevices*, vol. 11, no. 3, pp. 597-607, 2009.

[20] G. Mernier, N. Piacentini, T. Braschler, N. Demierre, and P. Renaud, "Continuous-flow electrical lysis device with integrated control by dielectrophoretic cell sorting.," *Lab on a chip*, vol. 10, no. 16, pp. 2077-82, Aug. 2010.

[21] P. Patel and G. Markx, "Dielectric measurement of cell death," *Enzyme and Microbial Technology*, vol. 43, no. 7, pp. 463-470, 2008.